frontiers | Frontiers in Endocrinology

TYPE Original Research
PUBLISHED 15 September 2022
DOI 10.3389/fendo.2022.963520

OPEN ACCESS

EDITED BY
Terry Francis Davies,
Icahn School of Medicine at Mount Sinai, United States

REVIEWED BY
Elisa Giannetta,
Sapienza University of Rome, Italy
Jaepyeong Cha,
Children's National Hospital, United States

*CORRESPONDENCE
Jian Wu
wo_doctor@163.com

†These authors have contributed equally to this work and share first authorship

SPECIALTY SECTION
This article was submitted to Thyroid Endocrinology, a section of the journal Frontiers in Endocrinology

RECEIVED 08 June 2022
ACCEPTED 31 August 2022
PUBLISHED 15 September 2022

CITATION
Wang B, Liu Z, Wu J, Liu Y, Wang P, Liu H, Wang H, Wang T, Wang J, Tang Y and Zhang J (2022) Bioelectrical impedance spectroscopy can assist to identify the parathyroid gland during thyroid surgery. *Front. Endocrinol.* 13:963520. doi: 10.3389/fendo.2022.963520

Bioelectrical impedance spectroscopy can assist to identify the parathyroid gland during thyroid surgery

Bin Wang[1†], Zaoyang Liu[2†], Jian Wu[1*], Ying Liu[3], Pin Wang[1], Hong Liu[1], Haobin Wang[1], Tielin Wang[1], Juan Wang[3], Yan Tang[4] and Junyan Zhang[5]

[1]Center of Breast and Thyroid Surgery, Department of General Surgery, Chengdu Third People's Hospital, Chengdu, China, [2]Department of General Thoracic Surgery, Chengdu Third People's Hospital, Chengdu, China, [3]Department of Ultrasound, Chengdu Third People's Hospital, Chengdu, China, [4]Department of Pathology, Chengdu Third People's Hospital, Chengdu, China, [5]Department of Computer Science, George Washington University, Washington, DC, United States

Objective: This study aimed to explore the effectiveness of bioelectrical impedance spectroscopy in the identification of parathyroid glands during thyroid surgeries.

Method: All patients who received thyroid surgeries at our department from January 2018 to February 2020 were recruited for this study. The bioelectrical impedance spectroscopy analyzer was applied to analyze on following tissues: thyroid tissues, lymph nodes, adipose tissues, and the tissues suspected to be parathyroid glands. Postoperative pathological reports were obtained as the golden standard to compare with the characteristic parameters obtained from bioelectrical impedance spectroscopy. The receiver operating characteristic curve analysis was used to assess the diagnostic value and the selection of the optimal threshold of these parameters from bioelectrical impedance spectroscopy.

Results: A total of 512 patients were enrolled in the study and 1898 specimens were measured by the bioelectrical impedance spectroscopy analyzer. There were significant differences in the parameter of f_c among parathyroid glands, thyroid tissues, lymph nodes, and adipose tissues (252.2 ± 45.8 vs 144.7 ± 26.1, 491.7 ± 87.4, 602.3 ± 57.3; P<0.001, P<0.001, P<0.001). The area under the receiver operating characteristic curves was 0.993 (95%CI: 0.989-0.996) for f_c. When the diagnostic criterion of f_c was set at 188.85 kHz~342.55 kHz, the sensitivity and specificity to identify parathyroid glands from lymph nodes and adipose tissues were both 100%. At this f_c, the sensitivity and specificity to identify parathyroid glands from thyroid tissues were 91.1% and 99.0%, respectively.

Conclusion: In conclusion, bioelectrical impedance spectroscopy could assist to differentiate parathyroid glands from peripheral tissues during thyroid surgeries.

KEYWORDS

bioelectrical impedance spectroscopy, thyroid, parathyroid gland, lymph node, adipose tissue

Introduction

The incidence of thyroid neoplasm was increased in the past decades (1–6), and thyroid neoplasm ranks in ninth place for incidence and fifth for the most frequently diagnosed cancer in women worldwide (7). Thyroidectomy with central neck dissection has been widely adopted for the treatment of thyroid neoplasm (8–11). However, postoperative hypoparathyroidism is one of the main complications and the incidence ranges from 4.6% to 51.9% (12–14). Although the postoperative transient hypoparathyroidism may recover in a few months, it results in extended hospitalization and a poor experience for patients (15). In more severe cases, permanent hypoparathyroidism may occur and result in low quality of life (15–17).

Hypoparathyroidism is usually caused by parathyroid gland injury from mechanical or thermal trauma, devascularization, or removal (18–20). The surgeons need to do their best to protect parathyroid function by preserving the parathyroid gland in site with sufficient blood supply. Nevertheless, devascularization or accidental removal of parathyroid glands does happen despite of meticulous dissection in surgeries. In such cases, parathyroid gland autotransplantation is important to save the function of those parathyroid glands that could not be preserved in site (21–23). It is indisputable that functional recovery of the autotransplanted parathyroid gland depends on its survival rate (24, 25). Therefore, it is critical to keep the parathyroid glands fresh before transplantation. Because ischemia may denature parathyroid glands, autotransplantation should be performed as soon as possible. Currently, it takes at least 30 minutes for intraoperative frozen biopsy to identify accidentally removed parathyroid glands. Therefore, there is an unmet medical need to find other feasible and reliable methods to identify parathyroid glands in a shorter time during thyroid surgeries.

Electrical impedance is the measurement of resistance that a circuit poses to an alternating current when voltage is applied (26). The electrical properties of biological tissues in various frequency ranges are determined by the cellular components and structures, which generate characteristic impedance spectra (27). It was reported that electrical capacities were different between benign and malignant tumors in the breast (28). Electrical impedance of biological tissues is a complex data that combines resistance and capacitance. It depends on the frequency of the alternating current voltage applied to the tissues and reflects the tissue characteristics of conductivity and charge storage properties (27).

Bioelectrical Impedance Spectroscopy (BIS) had been applied to identify malignant lesions since 1984 (29). This technique had been widely used for the diagnosis of various carcinomas (30–34) and for characterizing various tissues (35, 36). As for thyroid neoplasm, there were several studies focused on the diagnosis of thyroid nodules (37–40). Antakia and colleagues used the BIS technique to identify parathyroid glands in neck central compartment surgeries of a rabbit model (26). In a study of 54 patients, Hillary et al. suggested the feasibility of using the technique to aid parathyroid identification and preservation during thyroid and/or parathyroid surgery (41). In the current study, we included 512 patients to investigate the effectiveness of BIS in the identification of human parathyroid glands from other soft tissues during thyroid surgeries.

Patients and methods

Patients

This study recruited patients who underwent thyroid surgeries for various thyroid diseases at the Department of Thyroid and Breast Surgery of Chengdu Third People's Hospital from January 2018 to February 2020. The study protocol was approved by the Ethics Committee of Chengdu Third People's Hospital for the use of human subjects in research. All patients were provided written informed consent.

Methods

Different tissues exhibit different bioelectrical characteristics, thus bioimpedance can be adopted to characterize tissues. One popular method for tissue characterization is to fit spectroscopic data to the Cole-Cole model (42). The Cole equation models the behavior of permittivity and conductivity as a function of frequency:

$$Z(f) = R_\infty + \frac{R_0 - R_\infty}{1 + (j\frac{f}{f_c})^{1-\alpha}}$$

Where $Z(f)$ is the bioimpedance spectrum which is a vector of impedances; f is the spectrum frequency; R_∞ is the impedance at infinite frequency; R_0 is the impedance at direct current; f_c is the characteristic frequency of the tissue under analysis; α is the constant that characterizes the Cole distribution function. Data $Z(f)$ are fitted by nonlinear regression curve fitting. The resulting model parameter vector for each tissue is $m = [R_0; R_\infty; f_c; \alpha]$. The BIS analyzer (MScan1.0B, Sealand Technology, Chengdu, China; Figure 1) was used to measure the impedance of different specimens. The mechanism and measurement method of the BIS analyzer were also introduced by Du Z and Wu J (33, 34) and four parameters (R_0, R_∞, f_c, and α)were included in the analysis. The BIS analyzer was applied to the following tissues within two minutes after being resected during surgeries: thyroid glands, lymph nodes, adipose tissues, and tissues suspected to be parathyroid glands. Suspected parathyroid glands included true parathyroid glands that could not be preserved in site for surgical reasons and possible parathyroid glands confirmed to be lymph nodes and adipose tissues. Postoperative pathological reports were obtained by examining the paraffin sections and served as the golden standard to compare the BIS parameters.

Statistical analysis

The statistical analysis was performed with SPSS version 23.0 software (SPSS Inc, Chicago, IL). The results of parameters of BIS were expressed as mean ± standard deviation (SD) Unpaired Student's t-test was used to compare between groups. The receiver operating characteristic (ROC) curve analysis was used for the judgment of the diagnostic ability of the parameters and the selection of the optimal threshold value for diagnosis. The data of the tissues that were suspected to be parathyroid glands were used to verify the accuracy of the given diagnostic criteria. Statistical significance was set at $P<0.05$.

Results

A total of 512 patients were enrolled in this study, among which 436 patients underwent thyroid surgeries for carcinoma, 43 patients for thyroid adenoma, and 33 patients for multinodular goiter. During surgeries, 1898 specimens were analyzed by the BIS analyzer, among which 362 specimens were suspected as parathyroid glands and were further examined by the intraoperative frozen section biopsy (Table 1). The results of postoperative pathology examinations and BIS parameters of different tissues were listed in Table 2. There were significant differences in the parameter f_c between parathyroid glands and thyroid tissues, lymph nodes, and adipose tissues. Similar differences were obtained in the parameters of R_0/R_∞ and α between parathyroid glands and thyroid tissues, lymph nodes, and adipose tissues (Table 2).

We further analyzed the distribution of BIS parameters among different tissues. There were significantly different distributions in f_c among these tissues (Figure 2). The f_c of the parathyroid gland slightly overlapped with that of the thyroid tissues, but there was no overlap between parathyroid glands and lymph nodes or adipose tissues (Figure 2A). The distribution of parameters of R_0/R_∞ and α of parathyroid glands partly overlapped with that of thyroid tissues as well as that of lymph nodes (Figures 2B, C).

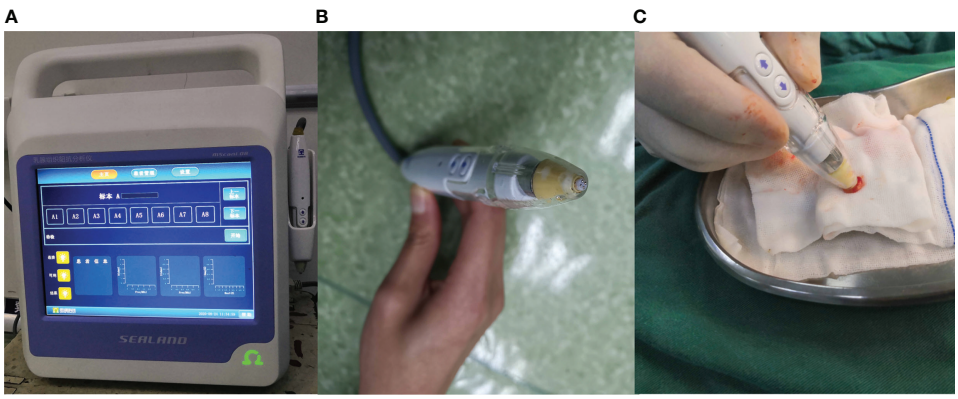

FIGURE 1
The Bioelectrical Impedance Spectroscopy analyzer. **(A)** analyzer. **(B)** probe. **(C)** the way of measurement.

TABLE 1 The relationship between patients and measured tissues.

Measured tissues	Patients (n)
1PG+1T+1LN+1AT	214
1PG+1T+1LN+2AT	17
1PG+1T+2LN+1AT	5
1T+1LN+1AT	172
1T+1LN+2AT	34
1T+2LN+1AT	70

PG, parathyroid gland; T, thyroid; LN, lymph node; AT, adipose tissue.

The area under the ROC curves was 0.993 (95%CI: 0.989-0.996; Figure 3A), 0.944(95%CI: 0.934-0.954; Figure 3B) and 0.948(95%CI: 0.938-0.958; Figure 3B) for f_c, R_0/R_∞, and α, respectively. According to these results, f_c was selected to further evaluate its diagnostic value. The mean value of f_c for parathyroid glands was larger than that for thyroid tissues (252.2 ± 45.8 vs 144.7 ± 26.1, P<0.001; Table 2), but was lower than that for lymph nodes and adipose tissues (252.2 ± 45.8 vs 491.7 ± 87.4, 602.3 ± 57.3; respectively, P<0.001, P<0.001; Table 2). The ranges of f_c did not overlap between parathyroid glands, lymph nodes, or adipose tissues (Figure 2A). The upper threshold of f_c was 342.55 kHz according to the ROC curve analysis (sensitivity 100%, specificity 100%). The lower threshold of f_c was 188.85 kHz (sensitivity 91.1%, specificity 99.0%; Figure 3A). The sensitivity and specificity were both 100% when the diagnostic criterion was used for identification of the tissues suspected to be parathyroid glands.

Discussion

In this study, we confirmed that the bioelectrical impedances were different among the parathyroid glands, thyroid tissues, lymph nodes, and adipose tissues. The f_c had some overlap between the parathyroid glands and thyroid tissues, but it had no overlap between parathyroids and lymph nodes or adipose tissues. The R_0/R_∞ and α of the parathyroid glands were the lowest among those of the four types of tissue.

A possible explanation is that different tissues consist of different types of cells or different proportions of similar cells. The bioelectrical impedances of tissues are determined by the properties of cells, the patterns of how these cells were constructed, and the cellular constituents such as lipid content and nuclear size, etc. Based on a similar theory, a multiparametric imaging approach can help to differentiate the parathyroid gland from the thyroid (43). In this study, the BIS parameters of the parathyroid glands were proved to be significantly different from those of other tissues. The types of cells in tissues might be responsible for the differences in BIS parameters. As described by Antakia et al., a thyroid gland is composed mostly of follicles that store thyroglobulin, lined by a single layer of epithelial cells with calcitonin secreting parafollicular cells scattered between follicles (26). In contrast, a parathyroid gland is composed of densely packed chief and oxyphil cells. Although fine-needle aspiration cytology confirmed that there is significant overlap in the cytomorphologic features of cells derived from the parathyroid and thyroid gland, the parathyroid was significantly associated with vascular proliferation, bare nuclei, intracytoplasmic fat vacuolation, high cellularity, and the absence of colloid (44, 45). Our data suggested that the compositions of lymph nodes and adipose tissue were different from that of the parathyroid gland and thyroid, which manifested in their distinctive BIS parameters.

From the view of thyroid surgeons, the greatest challenge of identifying parathyroid gland is to distinguish the parathyroid glands from the adipose tissue with naked eyes because of their similar appearance. Occasionally, lymph nodes might also be mistakenly identified as parathyroid glands. The use of marking techniques, such as carbon nanoparticle, methylene blue, and near-infrared imaging, provides some degree of help to distinguish these tissues (46–48). However, parathyroid glands are always accompanied or wrapped by adipose tissues, which causes the greatest challenge of identification.

In recent decades, more marking instruments have become available. Pasta and coworkers reported that Technetium ($Tc99^m$)-sestaMIBI was a helpful radiotracer for intraoperative localization of the parathyroid glands (49). Methylene blue was tested as a tracer for parathyroid identification, and the carbon nanoparticle was also used as a marking method (46). Carbon nanoparticle is a lymphatic tracer that stains and distinguishes the thyroid and lymphatic system, while the parathyroid and adipose tissues can be differentiated by being untinged. Near-infrared auto-fluorescence spectroscopy was also reported to be able to identify the parathyroid glands during thyroid surgeries

TABLE 2 The parameters of BIS of different tissue.

Parameters	PG (n = 236)	T (n=512)	LN (n=587)	AT (n=563)	P_T	P_{LN}	P_{AT}
f_c (kHz)	252.2 ± 45.8	144.7 ± 26.1	491.7 ± 87.4	602.3 ± 57.3	<0.001	<0.001	<0.001
R_0/R_∞	4.44 ± 0.57	5.49 ± 0.86	7.01 ± 1.17	12.55 ± 1.44	<0.001	<0.001	<0.001
α	0.56 ± 0.06	0.67 ± 0.07	0.72 ± 0.07	0.84 ± 0.07	<0.001	<0.001	<0.001

BIS, bioelectrical impedance spectroscopy; PG, parathyroid gland; T, thyroid; LN, lymph node; AT, adipose tissue; P_T: PG vs T; P_{LN} : PG vs LN; P_{AT} : PG vs AT.

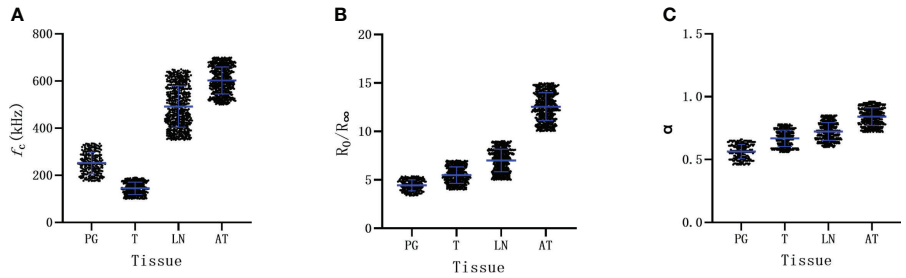

FIGURE 2
The distribution of Bioelectrical Impedance Spectroscopy parameters of different tissue. **(A)** parameter of f_c. **(B)** parameter of $R_0/R_\bullet$. **(C)** parameter of α. PG parathyroid gland, T thyroid, LN lymph node, AT adipose tissue.

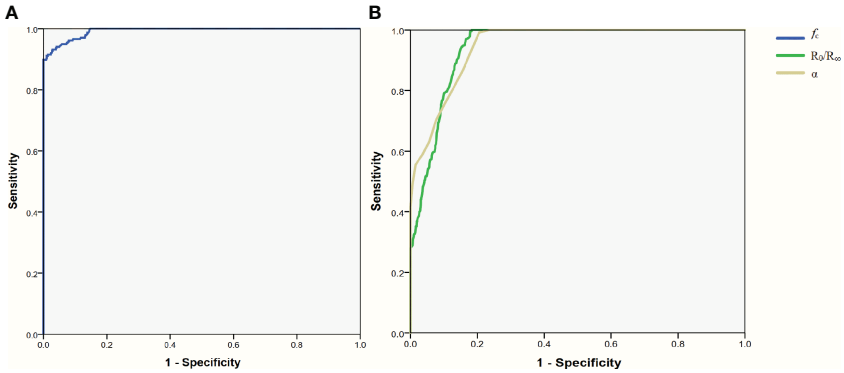

FIGURE 3
ROC curve for the parameters of Bioelectrical Impedance Spectroscopy. **(A)** parameter of f_c. **(B)** parameter of $R_0/R_\bullet$ and α. ROC receiver operating characteristic.

(48). However, such methods still require the experience of surgeons to distinguish parathyroid glands from adipose tissues.

During surgeries, surgeons often preserve the suspected parathyroid glands in site, but the nature of these suspected parathyroid glands may not be verified by pathology examination. In this study, we used a BIS analyzer to analyze those suspected parathyroid glands that could not be preserved in site or found in the intraoperative resected specimens. The natures of these suspected parathyroid glands were verified by intraoperative frozen pathological examination. When the parathyroid glands were confirmed by intraoperative frozen pathological diagnoses, they were transplanted into the sternocleidomastoid muscle. One of the most difficult issues is that intraoperative frozen pathological diagnoses always takes more than 30 minutes to get the reports. In contrast, BIS analyses only took a few minutes, and our results showed that the parameter f_c had perfect accuracy in distinguishing the parathyroid gland from lymph node and adipose tissue.

Our study opens new avenues for further research on this line. For example, the bioelectrical impedances could be sensitive to environment temperature and humidity. Whether these environmental changes may affect the cellular constituents such as lipid content and nuclear size needs further investigation. Some multicenter trials with larger samples are necessary to establish more reliable and accurate criteria.

Conclusions

In summary, this study indicates that the bioelectrical impedances vary from tissue to tissue. BIS is a potentially powerful tool to assist in identifying the parathyroid gland during thyroid surgeries. The results of this study would help reduce the incidence of postoperative hypoparathyroidism and thus help the recovery and quality of life of patients.

Data availability statement

The original contributions presented in the study are included in the article/supplementary material. Further inquiries can be directed to the corresponding author.

Ethics statement

The studies involving human participants were reviewed and approved by Ethics Committee of Chengdu Third People's Hospital. The patients/participants provided their written informed consent to participate in this study.

Author contributions

BW and JiW performed the research. All the authors contributed to the design of the work and the acquisition and interpretation of data. BW performed the statistical analysis and wrote the first draft. ZL revised the first draft. All authors contributed to the further drafts. JiW is the guarantor.

Funding

BW was supported by a nonprofit fund from China Health Promotion Foundation. JiW was supported by a grant from Scientific Research Fund of the Department of Science and Technology of Chengdu City (2015-HM01-00376-SF) and Science and Technology Program of Science & Technology Department of Sichuan Province (2015JY0190). The funding bodies had no role in the conception of the study, in the collection, analysis, and interpretation of data, in writing the manuscript and in the approval of the publication.

Acknowledgments

The authors thank the patients for their participation and the Sealand Technology (Chengdu) Limited for providing the BIS instrument.

Conflict of interest

The authors declare that the research was conducted in the absence of any commercial or financial relationships that could be construed as a potential conflict of interest.

Publisher's note

References

1. Leenhardt L, Bernier MO, Boin-Pineau MH, Conte Devolx B, Marechaud R, Niccoli-Sire P, et al. Advances in diagnostic practices affect thyroid cancer incidence in France. *Eur J Endocrinol* (2004) 150(2):133–9. doi: 10.1530/eje.0.1500133

2. Jung KW, Won YJ, Kong HJ, Oh CM, Seo HG, Lee JS. Cancer statistics in Korea: incidence, mortality, survival and prevalence in 2010. *Cancer Res Treat* (2013) 45(1):1–14. doi: 10.4143/crt.2013.45.1.1

3. Du L, Li R, Ge M, Wang Y, Li H, Chen W, et al. Incidence and mortality of thyroid cancer in China, 2008-2012. *Chin J Cancer Res* (2019) 31(1):144–51. doi: 10.21147/j.issn.1000-9604.2019.01.09

4. Dal Maso L, Lise M, Zambon P, Falcini F, Crocetti E, Serraino D, et al. Incidence of thyroid cancer in Italy, 1991-2005: Time trends and age-period-cohort effects. *Ann Oncol* (2011) 22(4):957–63. doi: 10.1093/annonc/mdq467

5. Qian ZJ, Jin MC, Meister KD, Megwalu UC. Pediatric thyroid cancer incidence and mortality trends in the united states, 1973-2013. *JAMA Otolaryngol. Head Neck Surg* (2019) 145(7):617–23. doi: 10.1001/jamaoto.2019.0898

6. Lim H, Devesa SS, Sosa JA, Check D, Kitahara CM. Trends in thyroid cancer incidence and mortality in the united states, 1974-2013. *JAMA* (2017) 317 (13):1338–48. doi: 10.1001/jama.2017.2719

7. Sung H, Ferlay J, Siegel RL, Laversanne M, Soerjomataram I, Jemal A, et al. Global cancer statistics 2020: GLOBOCAN estimates of incidence and mortality worldwide for 36 cancers in 185 countries. *CA Cancer J Clin* (2021) 71(3):209–49. doi: 10.3322/caac.21660

8. Haugen BR, Alexander EK, Bible KC, Doherty GM, Mandel SJ, Nikiforov YE, et al. 2015 American thyroid association management guidelines for adult patients with thyroid nodules and differentiated thyroid cancer: The American thyroid association guidelines task force on thyroid nodules and differentiated thyroid cancer. *Thyroid* (2016) 26(1):1–133. doi: 10.1089/thy.2015.0020

9. American Thyroid Association Guidelines Task Force, Kloos RT, Eng C, Evans DB, Francis GL, Gagel RF, et al. Medullary thyroid cancer: Management guidelines of the American thyroid association. *Thyroid* (2009) 19(6):565–612. doi: 10.1089/thy.2008.0403

10. Wells SAJr., Asa SL, Dralle H, Elisei R, Evans DB, Gagel RF, et al. Revised American thyroid association guidelines for the management of medullary thyroid carcinoma. *Thyroid* (2015) 25(6):567–610. doi: 10.1089/thy.2014.0335

11. American Thyroid Association Guidelines Taskforce on Thyroid Nodules Differentiated Thyroid Cancer, Cooper DS, Doherty GM, Haugen BR, Kloos RT, Lee SL, et al. Revised American thyroid association management guidelines for patients with thyroid nodules and differentiated thyroid cancer. *Thyroid* (2009) 19 (11):1167–214. doi: 10.1089/thy.2009.0110

12. Giordano D, Valcavi R, Thompson GB, Pedroni C, Renna L, Gradoni P, et al. Complications of central neck dissection in patients with papillary thyroid carcinoma: Results of a study on 1087 patients and review of the literature. *Thyroid* (2012) 22(9):911–7. doi: 10.1089/thy.2012.0011

13. Lee YS, Kim SW, Kim SW, Kim SK, Kang HS, Lee ES, et al. Extent of routine central lymph node dissection with small papillary thyroid carcinoma. *World J Surg* (2007) 31(10):1954–9. doi: 10.1007/s00268-007-9171-7

14. Pereira JA, Jimeno J, Miquel J, Iglesias M, Munne A, Sancho JJ, et al. Nodal yield, morbidity, and recurrence after central neck dissection for papillary thyroid carcinoma. *Surgery* (2005) 138(6):1095–100. doi: 10.1016/j.surg.2005.09.013

15. Bhattacharyya N, Fried MP. Assessment of the morbidity and complications of total thyroidectomy. *Arch Otolaryngol. Head Neck Surg* (2002) 128(4):389–92. doi: 10.1001/archotol.128.4.389

16. Bohrer T, Pasteur I, Lyutkevych O, Fleischmann P, Tronko M. [Permanent hypoparathyroidism due to thyroid cancer surgical procedures in patients exposed to radiation in the Chernobyl, Ukraine, nuclear reactor accident]. *Dtsch Med Wochenschr* (2005) 130(44):2501–6. doi: 10.1055/s-2005-918594

17. Polistena A, Monacelli M, Lucchini R, Triola R, Conti C, Avenia S, et al. Surgical morbidity of cervical lymphadenectomy for thyroid cancer: A retrospective cohort study over 25 years. *Int J Surg* (2015) 21:128–34. doi: 10.1016/j.ijsu.2015.07.698

18. Su A, Gong Y, Wu W, Gong R, Li Z, Zhu J. Does the number of parathyroid glands autotransplanted affect the incidence of hypoparathyroidism and recovery of parathyroid function? *Surgery* (2018) 164(1):124–9. doi: 10.1016/j.surg.2017.12.025

19. Su A, Gong Y, Wu W, Gong R, Li Z, Zhu J. Effect of autotransplantation of a parathyroid gland on hypoparathyroidism after total thyroidectomy. *Endocr Connect* (2018) 7(2):286–94. doi: 10.1530/EC-17-0313

20. Fahad Al-Dhahri S, Al-Ghonaim YA, Sulieman Terkawi A. Accuracy of postthyroidectomy parathyroid hormone and corrected calcium levels as early predictors of clinical hypocalcemia. *J Otolaryngol. Head Neck Surg* (2010) 39(4):342–8.

21. Lahey FH. The transplantation of parathyroids in partial thyroidectomy. *Surgery Gynecol Obstet* (1926) 62:508–9.

22. Palazzo FF, Sywak MS, Sidhu SB, Barraclough BH, Delbridge LW. Parathyroid autotransplantation during total thyroidectomy–does the number of glands transplanted affect outcome? *World J Surg* (2005) 29(5):629–31. doi: 10.1007/s00268-005-7729-9

23. Sokouti M, Montazeri V, Golzari S. The incidence of transient and permanent hypocalcemia after total thyroidectomy for thyroid cancer. *Int J Endocrinol Metab* (2010) 8(1):7–12.

24. Senapati A, Young AE. Parathyroid autotransplantation. *Br J Surg* (1990) 77 (10):1171–4. doi: 10.1002/bjs.1800771027

25. Kihara M, Miyauchi A, Kontani K, Yamauchi A, Yokomise H. Recovery of parathyroid function after total thyroidectomy: Long-term follow-up study. *ANZ J Surg* (2005) 75(7):532–6. doi: 10.1111/j.1445-2197.2005.03435.x

26. Antakia R, Brown BH, Highfield PE, Stephenson TJ, Brown NJ, Balasubramanian SP. Electrical impedance spectroscopy to aid parathyroid identification and preservation in central compartment neck surgery: A proof of concept in a rabbit model. *Surg Innov* (2016) 23(2):176–82. doi: 10.1177/1553350615607639

27. Dean DA, Ramanathan T, Machado D, Sundararajan R. Electrical impedance spectroscopy study of biological tissues. *J Electrostat* (2008) 66(3-4):165–77. doi: 10.1016/j.elstat.2007.11.005

28. Crile GW. Measurements of electrical capacity of benign and malignant tumors-clinical significance. *J Cancer Res* (1925) 9(3):388–90. doi: 10.1158/jcr.1925.388

29. Chaudhary SS, Mishra RK, Swarup A, Thomas JM. Dielectric properties of normal & malignant human breast tissues at radiowave & microwave frequencies. *Indian J Biochem Biophys* (1984) 21(1):76–9.

30. Smallwood RH, Keshtkar A, Wilkinson BA, Lee JA, Hamdy FC. Electrical impedance spectroscopy (EIS) in the urinary bladder: The effect of inflammation and edema on identification of malignancy. *IEEE Trans Med Imaging* (2002) 21 (6):708–10. doi: 10.1109/TMI.2002.800608

31. Aberg P, Birgersson U, Elsner P, Mohr P, Ollmar S. Electrical impedance spectroscopy and the diagnostic accuracy for malignant melanoma. *Exp Dermatol* (2011) 20(8):648–52. doi: 10.1111/j.1600-0625.2011.01285.x

32. Halter RJ, Schned A, Heaney J, Hartov A, Schutz S, Paulsen KD. Electrical impedance spectroscopy of benign and malignant prostatic tissues. *J Urol* (2008) 179(4):1580–6. doi: 10.1016/j.juro.2007.11.043

33. Du Z, Wan H, Chen Y, Pu Y, Wang X. Bioimpedance spectroscopy can precisely discriminate human breast carcinoma from benign tumors. *Med (Baltimore)* (2017) 96(4):e5970. doi: 10.1097/MD.0000000000005970

34. Wu J, Wang P, Tang Y, Liu H, Wang H, Zhang W, et al. Technical note: A new method to rapidly identify benign and malignant breast lumps through bioelectrical impedance spectroscopy. *Med Phys* (2019) 46(5):2522–5. doi: 10.1002/mp.13474

35. Rigaud B, Hamzaoui L, Frikha MR, Chauveau N, Morucci JP. *In vitro* tissue characterization and modelling using electrical impedance measurements in the 100 Hz-10 MHz frequency range. *Physiol Meas* (1995) 16(3 Suppl A):A15–28. doi: 10.1088/0967-3334/16/3a/002

36. Tao D, Adler A. *In Vivo*Blood characterization from bioimpedance spectroscopy of blood pooling. *IEEE Trans Instrum Meas* (2009) 58(11):3831–8. doi: 10.1109/tim.2009.2020836

37. Cheng Y, Fu M. Dielectric properties for differentiating normal and malignant thyroid tissues. *Med Sci Monit* (2018) 24:1276–81. doi: 10.12659/msm.908204

38. Stojadinovic A, Fields SI, Shriver CD, Lenington S, Ginor R, Peoples GE, et al. Electrical impedance scanning of thyroid nodules before thyroid surgery: A prospective study. *Ann Surg Oncol* (2005) 12(2):152–60. doi: 10.1245/ASO.2005.03.062

39. Nissan A, Peoples GE, Abu-Wasel B, Adair CF, Prus D, Howard RS, et al. Prospective trial evaluating electrical impedance scanning of thyroid nodules before thyroidectomy: Final results. *Ann Surg* (2008) 247(5):843–53. doi: 10.1097/SLA.0b013e318165c757

40. Zheng B, Tublin ME, Klym AH, Gur D. Classification of thyroid nodules using a resonance-frequency-based electrical impedance spectroscopy: A preliminary assessment. *Thyroid* (2013) 23(7):854–62. doi: 10.1089/thy.2012.0413

41. Hillary SL, Brown BH, Brown NJ, Balasubramanian SP. Use of electrical impedance spectroscopy for intraoperative tissue differentiation during thyroid and parathyroid surgery. *World J Surg* (2020) 44(2):479–85. doi: 10.1007/s00268-019-05169-7

42. Cole KS, Cole RH. Dispersion and absorption in dielectrics I. Alternating current characteristics. *J Chem Phys* (1941) 9(4):341–51. doi: 10.1063/1.1750906

43. Isidori AM, Cantisani V, Giannetta E, Diacinti D, David E, Forte V, et al. Multiparametric ultrasonography and ultrasound elastography in the differentiation of parathyroid lesions from ectopic thyroid lesions or lymphadenopathies. *Endocrine* (2017) 57(2):335–43. doi: 10.1007/s12020-016-1116-1

44. Dimashkieh H, Krishnamurthy S. Ultrasound guided fine needle aspiration biopsy of parathyroid gland and lesions. *Cytojournal* (2006) 3:6. doi: 10.1186/1742-6413-3-6

45. Kumari N, Mishra D, Pradhan R, Agarwal A, Krishnani N. Utility of fine-needle aspiration cytology in the identification of parathyroid lesions. *J Cytol* (2016) 33(1):17–21. doi: 10.4103/0970-9371.175490

46. Li Y, Jian WH, Guo ZM, Li QL, Lin SJ, Huang HY. A meta-analysis of carbon nanoparticles for identifying lymph nodes and protecting parathyroid glands during surgery. *Otolaryngol. Head Neck Surg* (2015) 152(6):1007–16. doi: 10.1177/0194599815580765

47. Su AP, Wei T, Gong YP, Gong RX, Li ZH, Zhu JQ. Carbon nanoparticles improve lymph node dissection and parathyroid gland protection during thyroidectomy: A systematic review and meta-analysis. *Int J Clin Exp Med* (2018) 11(2):463–73.

48. Liu J, Wang X, Wang R, Xu C, Zhao R, Li H, et al. Near-infrared auto-fluorescence spectroscopy combining with fisher's linear discriminant analysis improves intraoperative real-time identification of normal parathyroid in thyroidectomy. *BMC Surg* (2020) 20(1):4. doi: 10.1186/s12893-019-0670-x

49. Pasta V, Monteleone F, Del Vecchio L, Iacobelli S, Urciuoli P, D'Orazi V. Original technique for preoperative preparation of patients and intraoperative localization of parathyroid adenomas. *G Chir* (2015) 36(3):97–100. doi: 10.11138/gchir/2015.36.3.097